A Live Bioprobe for Studying Diatom-Surface Interactions

Fernando Terán Arce,* Recep Avci,* Iwona B. Beech,† Keith E. Cooksey,‡ and Barbara Wigglesworth-Cooksey‡
*Department of Physics, Montana State University, Bozeman, Montana, USA; †School of Pharmacy and Biomedical Sciences, University of Portsmouth, Portsmouth, United Kingdom; and ‡Department of Microbiology, Montana State University, Bozeman, Montana, USA

ABSTRACT Atomic force microscopy has been employed to compare the adhesion of *Navicula* species I diatoms to surfaces of a hydrophobic elastomer, Intersleek, and a hydrophilic mineral, mica. This was accomplished using tipless atomic force microscopy cantilevers functionalized with live diatom cells. Both surfaces were tested with the same diatom bioprobe. Force versus distance curves generated during these experiments revealed comparable cell adhesion strengths on Intersleek and mica, indicating that *Navicula* diatoms secrete extracellular polymeric substances with hydrophobic and hydrophilic properties. A statistical analysis of force curves was carried out and the average values of works of detachment of a diatom from Intersleek and mica surfaces were determined.

INTRODUCTION

The production of extracellular polymeric substances (EPS) by microorganisms is unequivocally accepted as a key mechanism facilitating irreversible cell attachment to inanimate surfaces in aqueous environments (Cooksey and Wigglesworth-Cooksey, 1995; Geesey, 1982). In particular, the interaction between EPS of marine microorganisms and fouling release coatings plays a significant role in the process of biofouling and is thus of major interest to the Navy and the maritime industry. It is now generally acknowledged that microbial EPS are a complex mixture of macromolecules such as proteins, polysaccharides, lipids, and nucleic acids and that their composition changes with microbial species, physiological status of the cells, and a wide range of environmental factors (Hoagland et al., 1993; Wingender et al., 1999).

Diatoms, which are a significant component of marine biofilms formed on all wetted and illuminated surfaces (Cooksey and Wigglesworth-Cooksey, 1995), are unicellular microalgae encased in a siliceous cell wall called the frustule. Diatoms exist in nature as benthic (attached to a sediment surface) and planktonic (free-floating) forms. Some diatoms interact with the substratum by releasing adhesive exopolymers through a distinct slit in the frustule called the raphe. In diatoms with bilateral symmetry such as *Navicula* species I, the raphe exists on the upper and lower surface of the diatom cell. Thus, either side of the diatom cell can attach to a substratum.

Bacteria are regarded as the primary colonizers of any submerged surface (Marshall, 1992); hence numerous investigations have focused on the chemical characterization of bacterial exopolymers and studies of their adhesive properties (Wingender et al., 1999; Zinkevich et al., 1996). In contrast, reports related to diatom EPS are infrequent (Cooksey and Wigglesworth-Cooksey, 1995) and knowledge about both the strength and the nature of forces between diatoms and the different surfaces which they colonize remains limited (Lind et al., 1997; Wetherbee et al., 1998).

Although exopolymers associated with benthic diatoms are known to comprise polysaccharides, proteins, and glycoproteins (Chiovitti et al., 2003; Staats et al., 1999), it is not apparent which of these macromolecules participate in the irreversible attachment of diatoms to a surface. It is also unclear to what extent the type of genera/species-specific adhesive macromolecules change with the physiological state of a diatom and the physicochemical properties of a surface. In particular, the effect of the conditioning layer formed by organic material present in seawater ought to be considered (Beech, 2000; Chamberlain, 1992; Compere et al., 2001; Schneider, 1997).

Characterization of the EPS produced by different genera of marine and freshwater diatoms based on morphology, serological analysis, and lectin interaction has led to positive identification of different types of exopolymers that can be broadly classified as 1), frustule EPS; 2), outer capsular EPS; 3), motility EPS; and 4), matrix EPS (Hoagland et al., 1993; Wigglesworth-Cooksey and Cooksey, 2005; Wustman et al., 1997).

Atomic force microscopy (AFM) studies have helped to determine some of the physical properties of EPS associated with surfaces of microbial cells. This has been achieved by measuring forces between as-received or functionalized AFM silicon nitride tips and living/dead microbial cells immobilized on different surfaces (Abu-Lail and Camesano, 2002; Callow et al., 2000; Dufrene, 2000, 2001; Razatos et al., 1998; Vadilli-Rodriguez et al., 2003; Van der Aa and Dufrene, 2002; van der Aa et al., 2001; Van der Mei et al., 2000). A number of investigators have followed this approach to demonstrate the complexity of species-de-

Submitted March 24, 2004, and accepted for publication September 15, 2004.

Address reprint requests to Prof. Recep Avci, Montana State University, Dept. of Physics, MSU Physics, EPS 264, Bozeman, MT 59717. Tel.: 406-994-6164; E-mail: avci@physics.montana.edu.

0006-3495/04/12/4284/14 $2.00

doi: 10.1529/biophysj.104.043307

pendent macromolecular composition and heterogeneous spatial distribution of different types of EPS on the diatom surface (Crawford et al., 2001; Higgins et al., 2002, 2003). However, relatively few studies have reported the use of AFM tips functionalized with microbial cells, termed bioprobes, for elucidating cell-material surface interactions (Bowen et al., 2001; Lower et al., 2001; Ong et al., 1999; Razatos et al., 1998). This latter AFM technique, known as biological force microscopy, offers great advantage when characterizing the interaction of microorganisms with surfaces varying in physicochemical properties immersed in varying physiological environments. Applying the same microbial cell as a bioprobe to carry out multiple measurements over a range of substrata eliminates the variability that is likely to arise due to differences between individual cells.

In marine environments the development of reliable strategies to prevent biofouling, defined as the attachment and settlement of marine organisms on inanimate surfaces, such as ship hulls, is of considerable interest to a variety of sectors. One of the common approaches, favored by the maritime industry and the U.S. Navy, is the use of minimally adhesive nontoxic coatings, such as the silicone elastomer Intersleek (Anonymous, 1999; Arce et al., 2003). Understanding the processes governing microbial cell attachment to such materials through the study of exopolymer-surface interactions is, therefore, of great importance when evaluating the antifouling performance of a coating.

Previous AFM studies reported the characterization of diatom EPS based on the interaction between the AFM tip and the surface of an immobilized diatom cell. Such approach allows mapping of the lateral distribution of forces on single cells and aids characterization of mechanical properties of exopolymer by stretching single EPS molecules. However, problems arise if an attempt is made to measure cell/surface interactions with materials different from that of the AFM tip (usually silicon nitride). Functionalizing the tip with materials other than self-assembled monolayers is, to a large extent, an uncontrolled process, as there are not many tools that can reliably determine the tip chemistry at its apex, where the interaction with the surface takes place. Furthermore, properties of some materials, such as antifouling coatings, may vary with thickness (Arce et al., 2003), a parameter that is difficult to measure on an AFM tip. It is also important to emphasize that the marine environment is an extremely corrosive medium and interaction of a thin coat grafted on an AFM tip can undergo serious changes as a result of tip-medium interactions, creating unknown complications in assessing the true tip-surface interactions. Finally, probing of the same cell with tips made of two different materials becomes complicated, as it requires the change of cantilevers. In contrast, a live cell attached to an AFM cantilever enables testing of different surfaces with the same bioprobe. Moreover, the large contact area of the bioprobe allows force measurements that are more statistically meaningful for assessing overall cell/surface interactions than the ones obtained with either functionalized or naked tips. It has been reported that in the latter case only 2% of the forces measured can be interpreted unambiguously (Marszalek et al., 2001). It should be noted that cell/surface interactions are additive, i.e., they don't average out, and can be detected either as a collection of small unbinding forces acting at different extensions or as a single unbinding event with a large force acting at a single extension.

Our study is the first of its kind to demonstrate the use of biological force microscopy for characterizing and comparing adhesion forces between extracellular polymers associated with surfaces of live cells of marine fouling diatoms of the *Navicula* genus and two surfaces of different physicochemical properties, namely mica and Intersleek, in a simulated marine environment. The method offers promise as a rapid screening system for evaluating antifouling properties of different materials.

MATERIALS AND METHODS

Diatom cultures

Cells of the common marine diatom *Navicula* sp. I were isolated from stabilized marine sediments and grown in ASP_2 medium as described elsewhere (Cooksey and Chansang, 1976). Diatoms were cultivated at 25°C under a 14/10-h light/dark cycle at 100 μE m^2/s from Cool-White fluorescent lights. Cultures were maintained in 5-ml glass tubes and subcultured every 4–5 weeks. Diatoms used for AFM experiments (7×10^6 cells/ml) were recovered from either the logarithmic or stationary growth phase. Cells harvested from both phases were 100% motile, as verified using light microscopy examinations.

Preparation of surfaces

International Paints (London, UK) Intersleek 425 constitutes the top of three coats used to protect immersed surfaces from corrosion and biofouling. Intersleek is a silicone elastomer with strong hydrophobic properties. Details about its preparation, chemical composition, and elastic properties have been given elsewhere (Arce et al., 2003). Briefly, the top coat is made of three parts: part A (finish gray), part B (converter), and part C (accelerator). Following the manufacturer's specifications, 15 volumes of part A, 4 volumes of parts B, and 1 volume of part C were mixed together. This mixture was sprayed onto the butyl alcohol-cleaned, stainless steel discs (12- or 15-mm diameter, 0.8-mm thickness, purchased from Ted Pella, Redding, CA) and used as AFM samples. The samples were stored in a clean environment for several months. Immediately before use, they were sonicated for 15 min in acetone, propanol, and methanol, respectively (all solvents used were of HPLC grade and purchased from Mallinckrodt Baker (Phillipsburg, NJ)). Thereafter they were left for 15 min in an ozone chamber (BioForce, Ames, IA) for further cleaning. After this treatment, the samples retained their hydrophobicity.

Muscovite mica (Ted Pella, Redding, CA) is an aluminum silicate containing potassium ions and its surface has hydrophilic properties. To be able to compare diatom adhesion forces to mica and Intersleek using the same diatom, a small square ($\sim 1 \times 1$ mm^2) of Intersleek was cut out with a scalpel from a paint sample and fixed with an epoxy glue (Permapoxy, Permatex, Marietta, GA) in the center of a circular (10-mm diameter) mica disk. After sonicating this mica/Intersleek assembly in acetone, propanol, and methanol (15 min in each solution), and leaving it in an ozone chamber for 15 min, the sample was fixed with Permapoxy to an AFM steel support.

Immediately before placing this support inside the AFM liquid cell, a 150- to 200-μl droplet of diatom suspension (prepared as described above) was pipetted onto the surface of mica/Intersleek assembly. The combination of all of these methods resulted in a partial coverage of the specimen surface by diatoms.

Atomic force microscopy

All measurements were performed with a Nanoscope III Extended Multimode AFM from Veeco Instruments (Santa Barbara, CA) with a vertical engagement (JV) 170 $\times$ 170 μm^2 scanner. Tipless silicon nitride probes (ULNC-NTNM type, purchased from Veeco) were used for measurements. These probes have four cantilevers with spring constants between 0.06 and 0.58 N/m. Adhesion measurements in force-volume mode were carried out in an array of 16 $\times$ 16 force versus distance curves uniformly distributed over an area of $\sim$50 $\times$ 50 μm^2. Tip velocities for these measurements were $\sim$3 μm/s, maximum contact forces exerted on the surface were typically between 1 and 6 nN, and the maximum piezo displacement was $\sim$3 μm. The time the diatom was allowed to interact with the surface during a measurement was $\sim$1 s. The maximum extension permissible in single force curves ($\sim$6 μm) is twice as much as that in force-volume mode ($\sim$3 μm). For this reason, single force curves were occasionally obtained to be able to probe a wider force-extension range. In this case, the tip was allowed to interact with the surface from 1 to 10 s and the tip velocities varied between 1 and 10 μm/s.

Attachment of viable diatoms to AFM cantilevers

Before actual AFM experiments, the stickiness and biocidal properties of a number of commercial glues were tested in sterile ASP_2 medium. The silicone-based room temperature vulcanizing adhesive sealant (RTV 66B, Permatex, Solon, OH) was identified as the best-performing glue, i.e., the one that had no effect on diatom viability and that did not cure too rapidly when exposed to air. The viability of diatoms after cell exposure to the glue was evaluated by observing changes in their color under a light microscope.

Two methods were used to attach *Navicula* diatoms to AFM tipless cantilevers. In the first method, a tipless cantilever in air was brought into contact with a very thin layer of the adhesive sealant and immediately withdrawn from its surface. Subsequent manipulations were carried out in sterile ASP_2 medium. The glue-conditioned cantilever was moved, with the help of the AFM stepper motor, toward one of the diatoms deposited on the surface of mica, and pressed gently against it for $\sim$2 s. The presence of the diatom on the cantilever was verified first in situ with the aid of an optical microscope integrated with the AFM instrument, and then using scanning electron microscopy (SEM) imaging (Fig. 1), as described below.

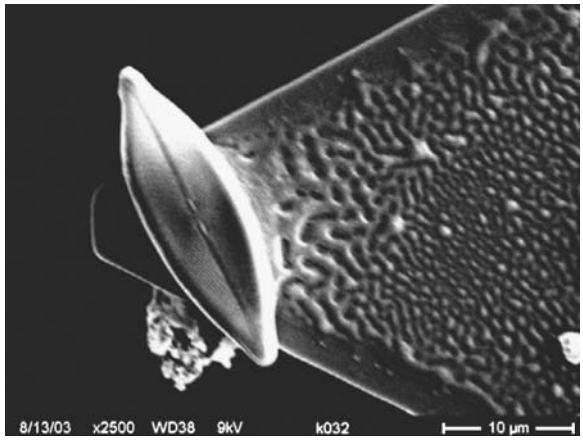

FIGURE 1 SEM micrograph of a single diatom cell attached with an epoxy glue to an AFM tipless cantilever using method 1, as described in the text.

In the second method, no glue was used and a tipless cantilever was simply pressed against one of the diatoms on the surface. This was performed under liquid in sterile ASP_2 medium. Besides using the optical microscope to verify the attachment of the cell to the cantilever we also used force measurements before and after cell attachment to make sure the cell was attached to the cantilever: Force versus distance curves were obtained with the tipless cantilever before its contact with the diatom surface and compared with the plots obtained after diatom attachment. Force curves acquired with the same cantilever differed considerably before and after diatom attachment.

The two methods (methods 1 and 2) gave comparable results in the essential features of the force curves. However, for measurements conducted over extended periods of time the use of glue was favored, as this method ensured both stability and viability of the bioprobes. With the second method diatoms were usually removed from the cantilever by the action of capillary forces when the cantilever was pulled out of the liquid environment at the end of an experiment.

Stability of measurements over time

To determine whether the EPS associated with the diatom probe was removed and released to the surrounding medium and/or deposited on the surface of mica or Intersleek during AFM experiments, force versus distance curves were collected and compared with each other as a function of time. Except for cases when unusually high loads ($\sim$1 μN) were applied accidentally during experiments, force versus distance curves for adhesive and very adhesive diatoms (as defined in the Results section) presented a large number of unbinding events, indicative of diatom presence and viability, over the time of measurements ($\sim$7 h). More importantly, adhesion forces and works of detachment (see below in this section for clarification of the terms) did not show a decreasing trend. If diatoms had lost EPS during experiments, decreasing values of the work of detachment would have been observed.

Scanning electron microscopy

Diatom-attached cantilevers were coated with a 15-nm gold layer using standard thin film coating equipment (Hummer VII, Anatech, Alexandria, VA) for scanning electron microscopy and imaged in a JEOL (Peabody, MA) 6100 SEM system. Fig. 1 shows an example of a diatom attached to a tipless cantilever imaged with SEM after performing adhesion measurements.

Statistical analysis of force versus distance curves

A MatLab (MathWorks, Natick, MA) code was written to analyze the force versus distance curves obtained in force-volume mode. This program identifies unbinding events by searching for all significant local minima, i.e., those clearly identifiable from noise according to their adhesion force values, in a retraction curve (Fig. 2 *b*). A noise filter was set, so that unbinding events with adhesion forces below a given threshold were not considered. A small fraction of force versus distance curves were identified as corrupt curves, e.g., due to excessive noise or ill-defined approach and/or retraction curves, and were excluded from the analysis. The area between the retraction curve and the zero force line was calculated using the trapezoidal rule for numerical integration. For each force versus distance curve, arrows pointing toward decreasing (increasing) values of the separation distance specify the approach (retraction) curve. Each retraction curve was analyzed by first finding the horizontal region in the approach curve. The zero force line was

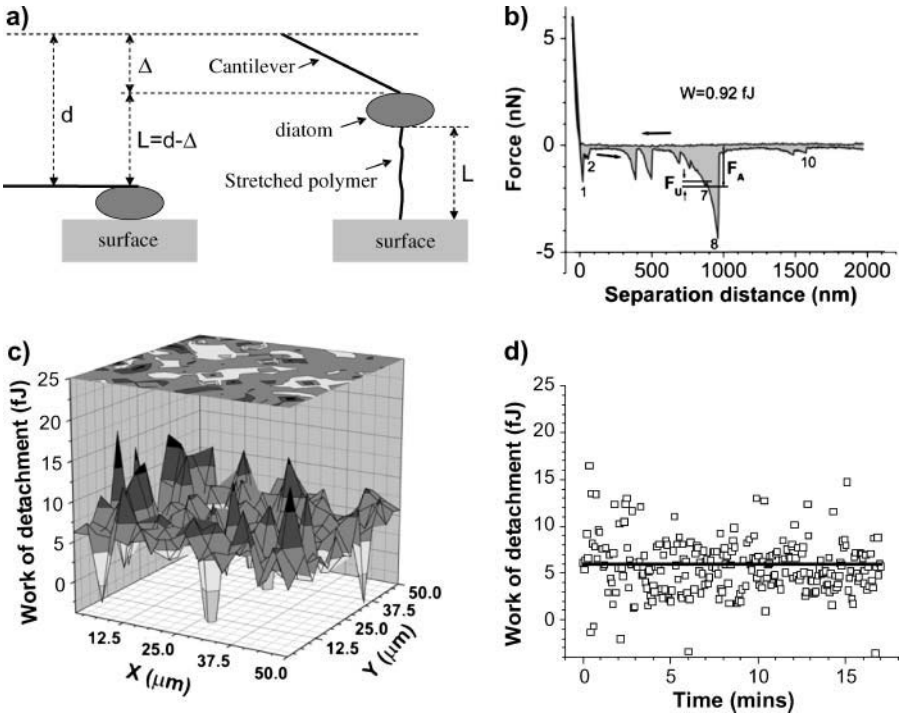

FIGURE 2 (*a*) The polymer length, $L = d - \Delta$, is calculated from the piezo displacement, d (called separation distance in the x axis of force versus distance curves), measured from the origin described in the text, and from the cantilever deflection, Δ. (*b*) An example of a force versus distance curve obtained on an Intersleek surface with a live diatom bioprobe. The work of detachment, W, is represented by the shaded area under the curve, the arrows indicate approach and retract directions. F_U and F_A show the unbinding and adhesion forces, respectively. (*c*) 3D mapping of the work of detachment obtained from a 16 × 16 array (spread over a 50 × 50 μm^2 area) of force versus distance curves in force-volume mode. At each (x,y) coordinate, the work of detachment (W) is plotted in the z axis. (*d*) Time representation of the information given in *c*. The start of data acquisition (time 0) corresponds to the $(x = 0, y = 0)$ point of the spatial array and the last point acquired (after 17 min in this example) corresponds to the force versus distance curve captured in the last point of the array, e.g., ($x = 50$ μm, $y = 50$ μm). The straight horizontal line in the graph represents the statistical average value of all points. Negative values are excluded from the analysis.

determined as the average value of points in the horizontal region. The intersection of this line with the retraction curve identifies the tip-surface contact point and defines the origin from which the polymer extensions and the magnitude of the adhesion (and unbinding) forces are measured in the retraction curve. For an unbinding event, the adhesion force corresponds to the magnitude of the force in the retraction curve measured from the zero force line. The corresponding separation distance, d, as shown in Fig. 2 *a*, represents the distance traveled by the piezo, from the origin of the curve (corresponding to the initial horizontal cantilever position in Fig. 2 *a*) to the unbinding event, whereby the cantilever deflection is denoted by Δ in the same figure. The polymer extension length, L, is simply given by the difference $L = d - \Delta$ as illustrated in Fig. 2 *a*.

Our analysis considers that diatoms are detached from the surface in a sequence of EPS unbinding events. Every time an individual exopolymer strand reaches its maximum extension length, L, and is released from the surface, the adhesion force decreases by an amount F_U, the unbinding force, that corresponds to the contribution of that particular exopolymer to the total adhesion force at the separation distance of the unbinding event (Fig. 2 *b*). The unbinding event, where the last bound exopolymer is finally detached from the surface and the adhesion force returns to zero, is known as the pull-off event (Abu-Lail and Camesano, 2002). This usually corresponds to the last well-defined adhesion peak in the retraction curve.

Polymer extensions and unbinding forces were found by applying and expanding the method used for the analysis of lengths and unbinding forces in antibody-antigen recognition events (Hinterdorfer et al., 1996). Adopting this approach, we estimated the contribution of individual exopolymers to the total adhesion force. For each force versus distance curve, the unbinding forces and the corresponding extension lengths are determined as depicted in Fig. 2, *a* and *b*. An unbinding force is determined from the difference between the forces corresponding to the local minimum and to the next local maximum in the direction of increasing values of the separation distance (Fig. 2 *b*). For example, for the unbinding event associated with the peak labeled ''7'' in Fig. 2 *b*, the adhesion force is ~1.89 nN and the corresponding unbinding force is calculated as the difference $F_U = 1.89$ nN $- 1.74$ nN $= 0.15$ nN, where the -1.74-nN value is the force associated with the local maximum to the immediate right of the unbinding event at peak ''7''. A complete analysis of the force curve shown in Fig. 2 *b* is summarized in Table 1, where we present a comparison of unbinding forces (F_U) with adhesion forces (F_A), and polymer extensions (L) with separation distances (d) for all unbinding events in the force curve of Fig. 2 *b*. Also shown in Table 1 are the relative variations $\delta = (d - L)/d$ and $\eta = (F_A - F_U)/F_A$. The values of δ and η suggest that there can be substantial variations in the adhesion and unbinding forces as well as in the polymer lengths associated with a live bioprobe interacting with a surface in a marine environment.

The shaded area between the negative portion of the retraction curve and the zero force line represents the work done by the cantilever against the external forces in order to detach the diatom bioprobe from the surface. This magnitude will be referred to as the ''work of detachment'' (W) per diatom throughout this article. Fig. 2 *c* shows an example of W mapping in a 50 × 50 μm^2 region of an Intersleek surface obtained in force volume mode using a diatom bioprobe. Since force versus distance curves are obtained one at a time, these maps can also be interpreted as a time sequence of W values (Fig. 2 *d*). Such data can be used to analyze variations of W over time and, as mentioned above, as an indicator of diatom viability throughout the experiment.

RESULTS

Stationary phase diatoms

Representative force curves

Fig. 3, *a–f*, shows different types of force versus distance curves obtained on Intersleek (Fig. 3, *a–c*) and on mica (Fig. 3, *d–f*) surfaces using *Navicula* diatoms harvested from the stationary phase. Regardless of the surface with which the bioprobes interacted, the majority of these curves display sequences of negative peaks that correspond

TABLE 1 List of polymer extensions, separation distances, unbinding forces, and adhesion forces for all unbinding events in Fig. 2 *b*

Peak No.	L (nm)	d (nm)	δ (%)	F_U (nN)	F_A (nN)	η (%)
1	6	71	92	1.32	1.71	23
2	50	107	53	0.51	0.64	20
3	374	439	15	1.44	1.60	10
4	485	549	12	1.40	1.57	11
5	685	743	8	0.56	0.86	35
6	754	814	7	0.36	1.08	67
7	858	925	7	0.15	1.89	92
8	924	1012	9	4.04	4.37	7
9	1483	1538	4	0.23	0.46	49
10	1570	1625	3	0.27	0.36	26

L, polymer extensions, d, separation distance, F_U, unbinding force, F_A, adhesion force. δ and η denote the percent values of $\delta = (d - L)/d$, and $\eta = (F_A - F_U)/F_A$.

to unbinding events of EPS macromolecules. One of the curves (Fig. 3 *f*) doesn't display any unbinding event, in spite of the large load with which the bioprobe compresses the surface. The hysteresis in this curve suggests that exopolymer associated with the surface of this bioprobe is compressed and deformed plastically during approach. The lack of adhesion forces indicates that this type of EPS does not contribute to cell attachment. Substantial variability in elongations and adhesion forces is seen from one force curve to another, irrespective of the type of material. The recorded adhesion forces range from fractions of nN to tens of nN and the measured exopolymer elongations reach up to 6 μm (the limit of our measurement) on both surfaces.

Work of detachment

Since the variability in adhesion characteristics depended primarily on the diatom used as a bioprobe, comparative measurements were performed on mica and Intersleek using the same diatom. To quantify the adhesiveness of diatoms for a given surface, the work of detachment per diatom was evaluated for 15 different diatoms. The results of three separate experiments, using diatoms 1, 2, and 3 (Table 2), recovered from the same culture (culture A) in the stationary phase of growth, are summarized in Fig. 4, *a–c*. Each point on the graph in Fig. 4 *a* represents the average value of 256 measurements, acquired in force-volume mode, on the surface of either mica or Intersleek. The origin of the time axis is the time at which the diatom was attached to a tipless cantilever in the simulated marine environment. These works of detachment are not statistically significantly different (Table 2) between Intersleek and mica, as their difference lies within the statistical error of the measurement (based on the values of standard deviations). However, the W value for individual diatoms varies considerably, ranging from 1.2 fJ to 2.4 fJ for diatom 1, from 0.4 fJ to 1.1 fJ for diatom 2, and from 0.6 fJ to 0.9 fJ for diatom 3, where fJ = femto-Joule. The lowest values are always recorded on mica and the highest ones on Intersleek. The work of detachment value differs depending on the individual diatom, regardless of the type of surface (Table 2, Fig. 4 *a*).

Temporal and/or spatial variations in the works of detachment for mica and Intersleek surfaces are depicted in Fig. 4, *b* and *c*, respectively. The straight horizontal line corresponds to the statistical average values which are plotted in Fig. 4 *a* (marked by *arrows*). Fig. 4, *b* and *c*,

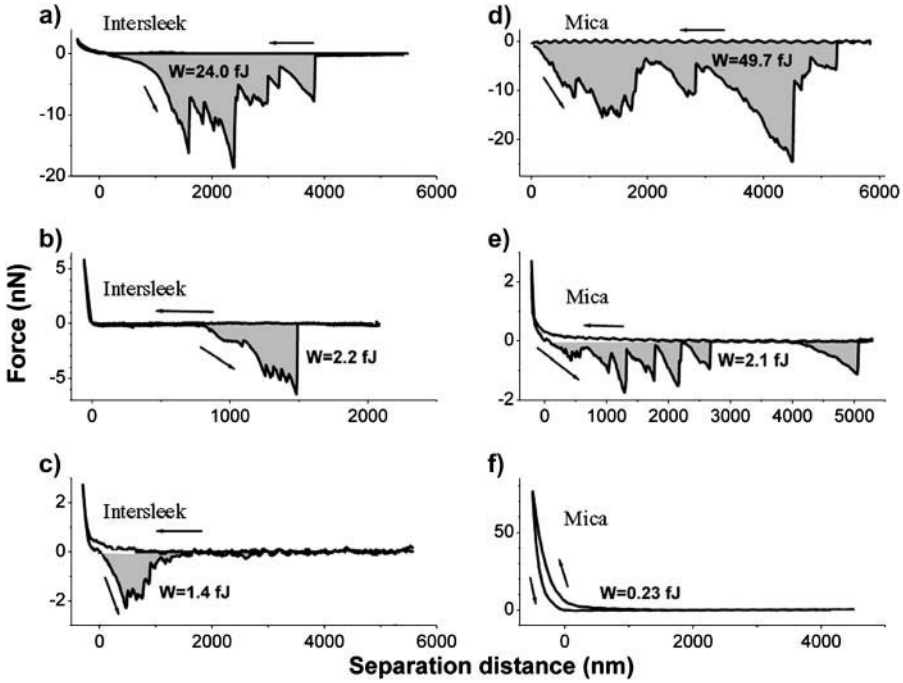

FIGURE 3 Representative force versus distance curves obtained with bioprobe diatoms in the stationary phase on Intersleek (*a–c*) and mica (*d–f*) surfaces. The work of detachment, W, is given in fJ units (10^{-15} J) for each curve. The arrows represent approach and retraction directions. All curves were obtained with different diatoms, with the exception of *c* and *e*, for which the same biprobe (diatom 1 in Table 2) was used. Diatoms are classified as very adhesive (*a* and *d*), adhesive (*b*, *c*, and *e*) or nonadhesive (*f*), according to their work of detachment values (*shaded areas*). Please note that adhesive and very adhesive diatoms usually display a large number of unbinding events.

TABLE 2 Summary of results for 15 different bioprobes

		Intersleek					Mica							
Diatom No.	Age (days)	W (fJ)	S. dev. (fJ)	F_{max} (nN)	No. of events	No. of curves	W (fJ)	S. dev. (fJ)	F_{max} (nN)	No. of events	No. of curves	Load (nN)	L_{max} (μm)	k (N/m)
1-A	7	2.2	0.7	2.1	7409	764	1.4	0.6	1.7	6425	746	13	3	0.06
2-A	9	1.1	1	3.7	2782	1613	0.9	0.6	1.9	3437	1521	6	3	0.06
3-A	7	0.9	0.4	3.7	174	246	0.8	0.4	3.1	733	744	6	3	0.32
4-B	18	23	11	28	206	18	—	—	—	—	—	27	6	0.12
4-B	18	9.7	6.8	18.5	70	13	—	—	—	—	—	1	6	0.12
4-B	18	5.9	2.7	9.7	1220	238	—	—	—	—	—	5	3	0.12
5-C	21	—	—	—	—	—	44	19	23	625	30	0.5	6	0.58
5-C	21	—	—	—	—	—	167	124	119	125	5	15	6	0.58
6-A	2	—	—	—	—	—	1.4	0.7	2.3	2545	252	6	3	0.06
7-B	29	—	—	—	—	—	1.0	0.3	1.8	2568	1043	1	3	0.06
8-B	18	1.3	0.9	7.1	271	248	—	—	—	—	—	5	3	0.12
9-D	7	—	—	—	—	—	1.7	0.5	3	238	18	23	3	0.58
10-D	7	—	—	—	—	—	10	7.4	10	250	12	278	5	0.58
11-E	2	0.8	0.3	14.4	1437	1280	—	—	—	—	—	15	3	0.32
12-F	2	10.8	7.6	11.4	313	61	28	29.6	11.9	189	34	2.5	6	0.12
13-F	2	—	—	—	—	—	13.1	8.7	10.3	341	31	1.5	6	0.12
14-G	15	0.6	0.5	3.5	926	425	—	—	—	—	—	6	2	0.12
15-G	15	1.0	0.8	5.5	308	241	—	—	—	—	—	6	2.2	0.58

F_{max} refers to the adhesion force higher than 95% of all adhesion forces measured under the same conditions of load and extension for a given diatom. W refers to the work of detachment defined in the text. L_{max} refers to the maximum extension in force versus distance measurements. Age refers to the age of the diatom culture. Seven cultures were used during experiments; they are specified by letters *A–G* in the first column of the table.

demonstrate that there is no apparent difference in spatial or temporal distribution of the work of detachment values and that no obvious trend can be observed on either of the surfaces. However, considerable fluctuations in the work of detachment values are noted from one force versus distance curve to the next, irrespective of the surface.

To aid data analysis, diatoms were arbitrarily classified as nonadhesive, adhesive, and very adhesive. Bioprobes referred to as ''nonadhesive'' are characterized by work of detachment values of <0.5 fJ. The force versus distance curve in Fig. 3 *f* represents this class of diatoms. The values for bioprobes that are termed ''very adhesive'' are at least 9 fJ (e.g., Fig. 3, *a* and *d*). These values relate to single force-distance measurements extending up to 6 μm separation. Diatoms for which the work of detachment value ranges from 0.5 fJ to 9 fJ are categorized as ''adhesive'' (Fig. 3, *b*, *c*, and *e*). Diatoms representing these three classes were found in all studied cultures.

It must be noted that for force curves obtained from a single location, the piezo has a maximum extension of 6 μm (e.g., curves in Fig. 3), whereas for force-volume measurements the maximum extension is 3 μm. Therefore, the work of detachment values calculated for adhesive or very adhesive diatoms are typically higher for curves obtained from a single location. Fig. 3 *e* provides an example of a force versus distance curve obtained from a single location using an adhesive diatom as bioprobe (diatom 1 in Fig. 5, and in Table 2) on the surface of mica. The work of detachment calculated from this plot is 2.2 fJ and is comparable with the average value of $\sim$1.5 fJ obtained for the same diatom from force-volume measurements (Fig. 4 *a*).

Statistical analysis of force versus distance curves

Adhesive diatoms

The statistical evaluation of force versus distance curves, obtained from single locations or acquired in force-volume mode, is based on the analysis of the number of unbinding events and polymer extension values. Irrespective of the type of surface, the average number of the unbinding events per force plot is, in general, highly dependent on the individual diatom used in the experiment. The number of such events per curve ranges from one event or no event for nonadhesive diatoms (e.g., Fig. 3 *f*) to more than 10 events for ''very adhesive'' diatoms (e.g., Fig. 3 *d*).

The distributions of unbinding and adhesion forces, as well as their extensions, are displayed in Fig. 5, *a–f*, where *a–c* correspond to the results obtained with diatom 1 and *d–f* with diatom 2. A total of four force-volume measurements, each with 256 force curves, were acquired. The total number of events is listed in Table 2 and is described in the figure caption (Fig. 5). Open bars correspond to mica and the shaded bars to Intersleek. Although the measured values are highly diatom-dependent, some similarities are observed between the two surfaces.

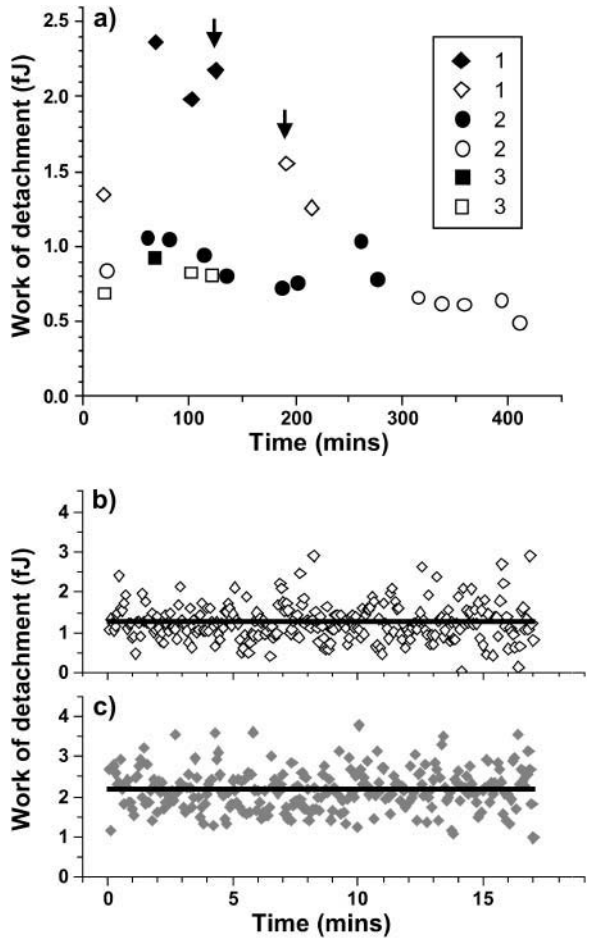

FIGURE 4 (*a*) Works of detachment as a function of time for three experiments in which the same diatom was used to probe Intersleek (*closed symbols*) and mica (*open symbols*). Each point represents the average value of 256 measurements such as those (indicated by *arrows*) displayed in *b* and *c* for mica and Intersleek, respectively. The numbers 1–3 assigned to the diatoms refer to the corresponding numbers in Table 2. The time origin in panel *a* refers to the instant the diatom was attached to the cantilever.

Irrespective of the diatom, the unbinding force distributions (Fig. 5, *a* and *d*) for both surfaces have maxima in the 0.1–0.4 nN range, although more such events are recorded on mica than on Intersleek. No appreciable difference between Intersleek and mica is seen in the distribution of unbinding forces >0.5 nN. The adhesion force distribution demonstrates that for both diatoms the maxima in the adhesion force distributions (Fig. 5, *b* and *e*) lie below 1 nN and that within this force range a larger fraction of events is obtained on mica.

The distribution of polymer extensions is presented in Fig. 5, *c* and *f*, for diatoms 1 and 2, respectively. Similar patterns are seen for both bioprobes. A considerable fraction of adhesion events with high extension values (≥ 1 μm) is observed on each surface. Although 65% of all events measured with diatom 1 have extension values >1 μm for Intersleek, 56% fall into this range in the case of mica. For diatom 2, extension values >1 μm represent 83% of all events on Intersleek and 70% of those on mica. These plots suggest that for a given diatom, the length distributions associated with mica and Intersleek are similar to each other, whereas for a given surface, different diatoms produce different extension distributions.

Very adhesive diatoms

To be able to probe larger polymer extensions than those available in force-volume measurements, single force curves were performed using diatoms 4 and 5 (see Table 2 for details). Fig. 6, *a* and *b*, shows the extension and unbinding force distributions for the very adhesive diatom bioprobes. From Table 2 it is apparent that for this class of diatoms, adhesion forces and works of detachment depend on the maximum load applied. The largest adhesion force measured on Intersleek was 38 nN, whereas the maximum adhesion force measured on mica reached 250 nN. To avoid isolated events, however, the quantity listed as F_{max} in Table 2 represents the adhesion force that was >95% of all adhesion forces measured for a given maximum load applied to the surface (Load in Table 2).

The unbinding force distributions are similar for both surfaces (Fig. 6 *a*). An exception is the region with force values close to 1 nN, where the fraction of unbinding events on mica is twice as high as the one recorded on Intersleek. The polymer extension distributions vary considerably between the two surfaces. It should be noted that the comparison of extensions is carried out between two different diatoms; hence, these results are in general agreement with those presented in Fig. 5. The position of the maximum events recorded on mica differs from that on Intersleek (Fig. 6 *b*). While a well-defined maximum is observed at 2500 nm for Intersleek (*shaded bars*), two less defined maxima (at 1600 nm and 3000 nm) appear on mica (*open bars*). Fig. 7 shows the distributions of unbinding forces versus polymer extensions for adhesive (Fig. 7, *a* and *c*)—and very adhesive (Fig. 7, *b* and *d*)—diatoms on Intersleek (*closed symbols*) and mica (*open symbols*). Each point in the plot represents an unbinding event in a force versus distance curve. The plots demonstrate that there is an order of magnitude difference in the values of unbinding forces between adhesive and very adhesive diatoms, irrespective of the surface. If we arbitrarily define a 1 nN force as a large unbinding force at the molecular level (~1 nN is typically the force required to break a covalent bond), the majority of the unbinding forces observed for the adhesive diatoms stay at <1 nN, whereas the majority of the forces for the very adhesive diatoms remain above this value.

Log phase diatoms

Force versus distance curves (Fig. 8, *a–d*) with diatoms recovered from the log phase displayed similar unbinding

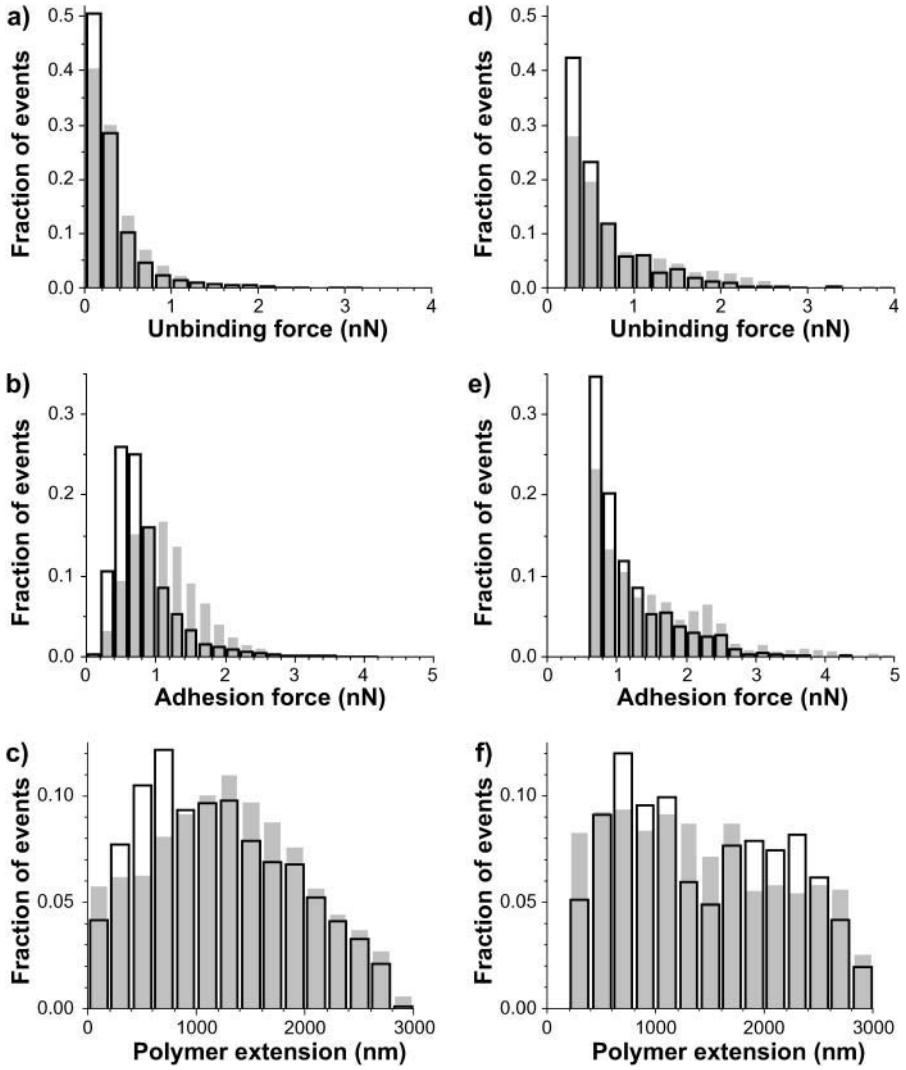

FIGURE 5 Histograms of unbinding forces (*a* and *d*), adhesion forces (*b* and *e*), and polymer extensions (*c* and *f*) for diatoms 1 (*a–c*) and 2 (*d–f*) in Table 2. For diatom 1, 6425 events were detected in 746 force curves analyzed for mica (*open bars*). In the case of Intersleek (*shaded bars*) the corresponding numbers were 7409 events in 764 force curves. For diatom 2, there were 3437 events in 1521 force curves for mica and 2782 events in 1613 force curves on Intersleek. Due to larger experimental noise during measurements performed with diatom 2 than with diatom 1, a higher force threshold was used in the analysis of measurements with diatom 2.

characteristics to those found in diatoms from the stationary phase. Force curves obtained with very adhesive (Fig. 8, *a* and *c*) and adhesive (Fig. 8 *d*) diatoms showed several unbinding peaks. The corresponding curves obtained with nonadhesive diatoms either did not display any unbinding peak or displayed only a shallow peak. The works of detachment values measured for log-phase *Navicula* cells on mica or Intersleek were comparable to those measured for diatoms in the stationary phase. A comparison of the works of detachment on Intersleek for diatoms 4 (stationary phase) and 12 (log phase) in Table 2 shows similar values. Although, according to our classification, these values fall into the ''very adhesive'' category, a similar trend is observed for adhesive diatoms. A discussion of whether these coincidences between log-phase and stationary-phase diatoms are statistically meaningful for large diatom populations is beyond the scope of this article.

Analogous to the unbinding force distribution for adhesive diatoms in the stationary phase (Fig. 5 *a*), the corresponding distribution for log-phase diatoms on mica shows that the majority of unbinding forces are in the 0–0.4 nN range (Fig. 9, *a* and *b*). Furthermore, the maximum of the length distribution is located between 1.6 and 1.8 μm (Fig. 9 *c*).

Fig. 9, *d–f*, presents the statistical distributions on mica and Intersleek obtained with the same very adhesive diatom (diatom 12 in Table 2) in the log phase. For this experiment, the first surface tested was Intersleek. In contrast to the stationary-phase diatoms, the majority of events in the unbinding force distribution has forces <1 nN, as seen in the unbinding force distributions of log-phase diatoms on mica (Fig. 9, *d* and *e*). The length distribution plot (Fig. 9 *f*), presents a well-defined maximum around 2100 nm, which is not very far from the position of the maximum found in the length distribution for very adhesive diatoms in the stationary phase (Fig. 6 *b*). Similar to the length distribution for diatoms in the stationary phase, several less well-defined maxima appear in the length distribution of the log-phase diatoms on the mica surface (Fig. 9 *f*).

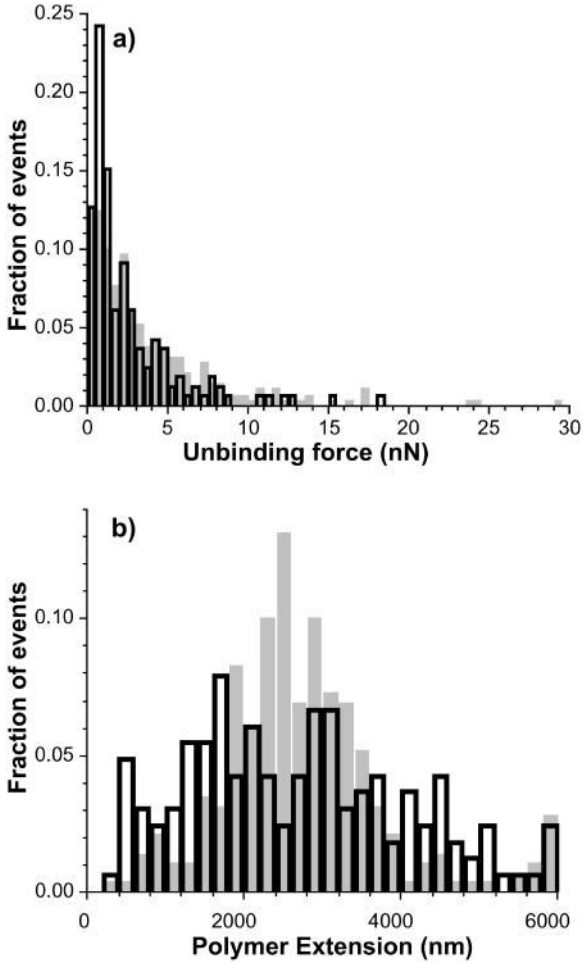

FIGURE 6 Unbinding force and polymer extension histograms for the very adhesive bioprobes. Data were extracted from single force curves extending up to 6 μm. Shaded bars correspond to measurements on Intersleek (diatom 4 in Table 2) and open bars to measurements on mica (diatom 5 in Table 2). For Intersleek, 276 adhesion events were detected in 31 force curves, whereas for mica, 841 events were detected in 38 force curves.

DISCUSSION

The process of microbial cell adhesion to inanimate surfaces is a complex phenomenon governed by a wide range of environmental and physiological parameters. It is unequivocally accepted that diatom attachment to a surface is facilitated by the secretion of adhesive exopolymers (Cooksey, 1981; Higgins et al., 2002). It must be emphasized that the composition and yield of these polymers not only change with diatom species, but also depend on the growth stage of a given diatom (Wigglesworth-Cooksey et al., 2001). Over the life cycle of a diatom cell, i.e., from the adaptation, or nongrowth (lag), phase, through the actively reproductive, logarithmic (log) phase until the nonreproductive stationary phase, several distinct types of EPS, e.g., motility, outer capsule, and matrix EPS, could participate in the adhesion process. However, the initial adhesion of a diatom cell to a surface is most likely to involve the motility and capsular polymers (Wetherbee et al., 1998; Wigglesworth-Cooksey and Cooksey, 1992).

Physiological studies have shown that most diatoms release copious amounts of EPS during the stationary phase and, generally, much smaller amounts during the logarithmic phase (Hoagland et al., 1993). AFM investigations of the adhesive properties of exopolymers are usually performed with the former diatoms to ensure the presence of adhesive material. The fact that 100% of the cells of *Navicula* sp. showed motility regardless of the growth phase makes it an attractive model organism for the study of EPS-surface interactions (Wigglesworth-Cooksey and Cooksey, 2005).

It has also been reported that, for some diatoms, adhesive properties of their EPS are unrelated to the amount of exopolymer produced (Becker, 1996), therefore suggesting that it is the chemical composition of EPS and not its yield that is important in the cell attachment process.

As already stated, the production of exopolymers by individual cells depends on the type of the diatom species and the growth conditions. Similar to bacteria, diatoms secrete a whole range of EPS throughout their life cycle. The production of the EPS is, however, a dynamic process and the exopolymer is frequently released into the bulk liquid. The EPS loss from the bacterial cell surface (shedding) is unequivocally accepted (Beech et al., 1999) and the same process is likely to apply to diatom cells (Wigglesworth-Cooksey and Cooksey, 2004, 2005). The type of EPS macromolecules associated with the surface of an individual diatom is, therefore, subject to temporal variations due to the reoccurring loss of the EPS material. The evidence that diatoms from the same stage of growth and from the same culture exhibit different adhesion characteristics supports the existence of such temporal variations. It is perhaps worth noting that the observed differences in the adhesiveness of diatoms from the same growth phase is independent of the experimental procedure as the nonadhesive diatoms remained nonadhesive, regardless of the number of measurements taken and the type of a substratum tested with such bioprobes. Likewise, adhesive or very adhesive bioprobes retained their properties throughout experiments involving multiple measurements.

No significant difference, i.e., beyond the statistical error contained in the standard deviation, in the work of detachment values was seen for *Navicula* cells between mica and Intersleek, A similar phenomenon has been reported for the marine diatom *Amphora coffeaeformis* (Becker, 1996). This study showed that the strength of attachment of *A. coffeaeformis* to glass was equal to that measured on hydrophobic polytetrafluorethylene. Another study (Characklis and Cooksey, 1983), also with *A. coffeaeformis,* reported similar results, but emphasized the minimum in adhesion that occurred at intermediate wettability of the surface.

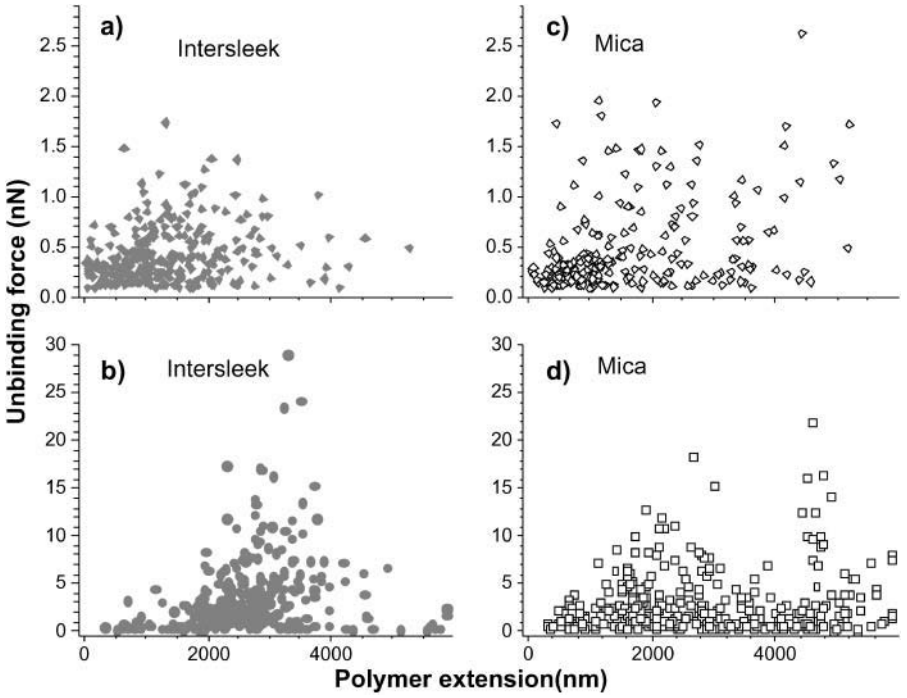

FIGURE 7 Unbinding force versus polymer extension plots for adhesive (*a* and *c*) and very adhesive (*b* and *d*) diatoms on Intersleek (*closed symbols*) and mica (*open symbols*). Diatom 1 was used for plots *a* and *c*, and diatoms 4 and 5 were used for plots *b* and *d*, respectively. For diatom 1, 32 curves were analyzed for both surfaces. There were 297 events detected for Intersleek and 223 for mica. For the very adhesive diatoms, the same force curves as in Fig. 6 were used to construct the plots in *b* and *d*.

Using the same adhesive *Navicula* bioprobe recovered from the stationary phase, values of the adhesion forces recorded on Intersleek were slightly higher than those measured on mica (but still comparable within the statistical error). This observation is in agreement with a study that employed patterned self-assembled monolayers to demonstrate that *Amphora coffaeformis* diatoms adhered more strongly to hydrophobic surfaces than to hydrophilic self-assembled monolayers (Finlay et al., 2002). In contrast, the same experiment performed with a very adhesive log-phase bioprobe (diatom number 12 in Table 2) showed a higher, but not significantly different, work of detachment value on mica; regardless of whether *W* is greater on mica or Intersleek, the high values obtained on both Intersleek and

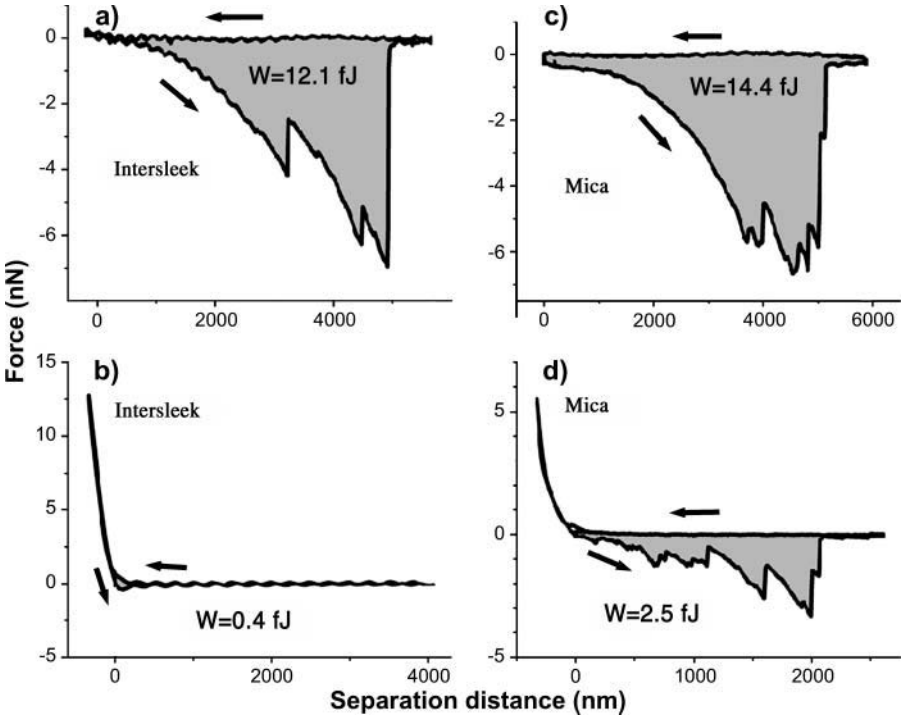

FIGURE 8 Force versus distance curves between log-phase diatoms and Intersleek (*a* and *b*) or mica (*c* and *d*) surfaces. Analogous to force curves with stationary-phase diatoms (Fig. 3), log-phase diatoms display very adhesive, adhesive, or nonadhesive characteristics. The force curves in *a* and *c* were obtained with the same diatom (number 12 in Table 2) and *b* and *d* were acquired with diatoms 11 and 6, respectively.

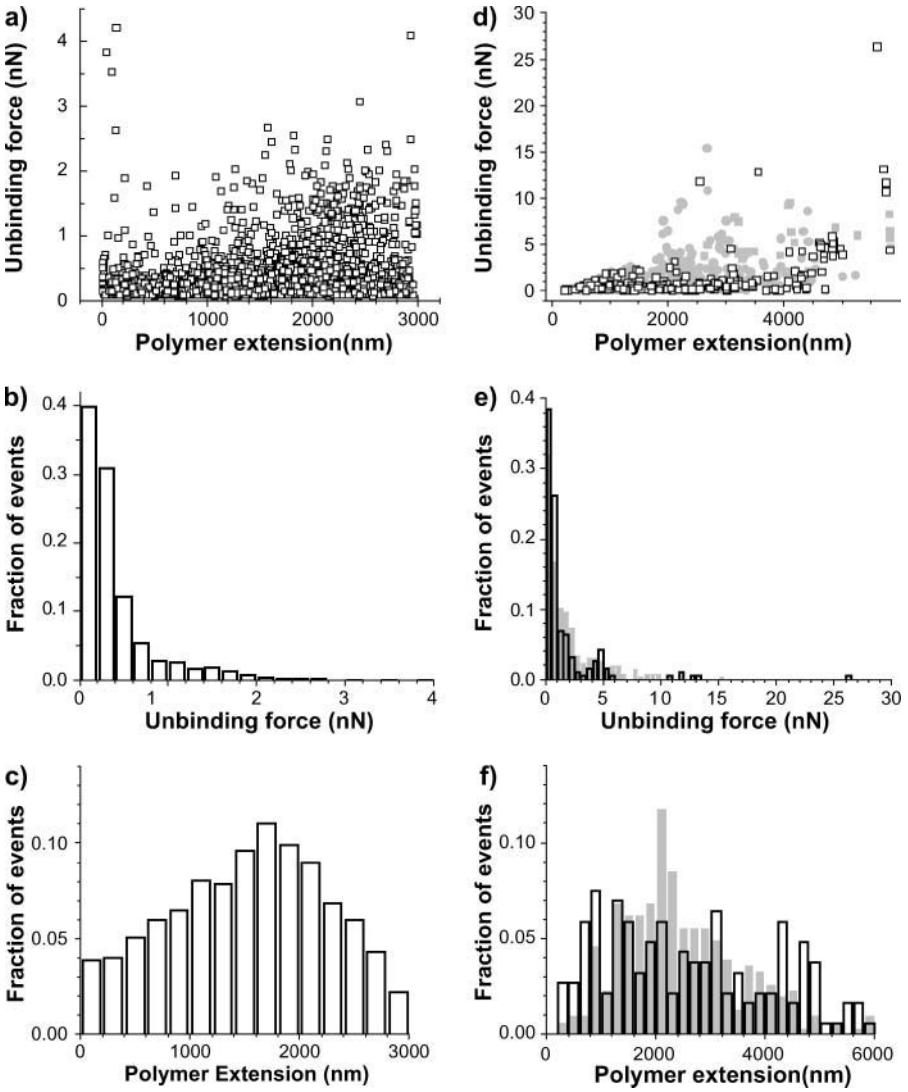

FIGURE 9 Unbinding force versus polymer extension plots (*a* and *d*), unbinding force (*b* and *e*), and polymer extension (*c* and *f*) histograms for an adhesive (*a–c*) and a very adhesive (*d–f*) log-phase diatom on mica (*open symbols*) and Intersleek (*closed symbols*). These data are similar to that shown in Figs. 5 and 7, obtained with stationary-phase diatoms.

mica surfaces with the same diatom indicate the involvement of chemically different EPS macromolecules.

For adhesive diatoms in the stationary phase, events with forces $>\sim 1$ nN occur in a narrower range of polymer extensions for Intersleek than for mica surfaces (Fig. 7, *a* and *c*). This suggests that EPS macromolecules of comparable lengths are responsible for cell-surface interaction on Intersleek surfaces, whereas exopolymers having a wider range of lengths interact with mica. A similar phenomenon is observed for very adhesive diatoms (diatoms 4, 5, and 12 in Table 2). In this case, most adhesion events are confined to a region between 2 and 4 μm for Intersleek, whereas for mica these events are visible in two or more length regions (Figs. 6 *b* and 9 *f*).

Force versus distance curves (Figs. 3 and 8) also revealed the presence of multiple unbinding forces at different separation distances, further supporting the evidence that for a given diatom, EPS macromolecules varying in chemical composition and/or molecules with similar chemical composition but of different length are involved in cell adhesion to different substrata. Whether these macromolecules belong to the same category, i.e., are polysaccharides, proteins, nucleic acids, or glycoproteins, or consist of a mixture, is a matter of speculation. A few AFM studies have demonstrated that many biopolymers (proteins, polysaccharides, and DNA) produce unique molecular fingerprints when mechanically stretched (Marszalek et al., 2001). However, identification of individual biopolymers or several macromolecules interacting with the tip in complex mixtures, such as EPS, based on such fingerprints, remains unreliable.

It has been reported that EPS secreted from the raphe region of the diatom *Craspedostauros australis* in stationary phase consists of polysaccharide-rich strands of macromolecules that aid cells in their attachment to the substrate and also contribute to their motility (Higgins et al., 2002; Wetherbee et al., 1998). This exopolymer was characterized by high adhesion forces of up to 60 nN and elongation forces of up to 10–15 μm (Higgins et al., 2002). Another AFM

study, of exopolymer secreted by the marine green algae, *Enteromorpha linza*, revealed that it consisted of glycoprotein with highly adhesive properties. The maximum force values for this EPS were up to 46 nN (Callow et al., 2000); however, polymer extensions did not exceed 400 nm. In comparison with the above studies, the highest value of the adhesion forces recorded for *Navicula* sp. I (>250 nN on mica) was higher than that reported for *C. australis* or for *Enteromorpha*; however, the polymer extensions (measured within the limitations <6 μm in our system) for *Navicula* were comparable with the ones recorded for *C. australis*. The EPS secreted by cells of *Navicula* sp. I on glass leaves characteristic footprints that are reactive with lectin Concanavalin A (Wigglesworth-Cooksey and Cooksey, 2005). This indicates that *Navicula* EPS contains macromolecules composed of hydrophilic carbohydrates, such as glucose, mannose, and N-acetylglucosamine, for which Concanavalin A is specific. As discussed below, macromolecules rich in these sugars would facilitate attachment of *Navicula* to glass surfaces, but not to Intersleek.

It is acknowledged that although EPS produced by some bacteria facilitate cell adhesion to hydrophilic surfaces, exopolymers of other bacteria show a preference for hydrophobic materials (Bakker et al., 2003). Moreover, certain bacteria, such as, e.g., *Vibrio proteolytica,* have separate adhesion mechanisms, i.e., different macromolecules are involved in EPS-surface interaction, depending on the wettability (or surface energy) of the colonized material (Paul and Jeffrey, 1985). Hydrophobic polysaccharides, proteins, and lipids present in microbial EPS have all been implicated in microbial cell adhesion to hydrophobic (low surface energy) substrates, whereas acidic and neutral polysaccharides have been proposed to facilitate attachment to hydrophilic (high surface energy) materials (Neu and Marschall, 1991; Wigglesworth-Cooksey and Cooksey, 1992). Exopolymers composed of different macromolecules, or even the same type of macromolecules that have hydrophilic and hydrophobic regions (e.g., hydrophobic polypeptides and hydrophilic saccharides on glycoproteins) can adhere to a wide range of surfaces (Becker, 1996). Our results indicate that either different EPS macromolecules, different segments on these macromolecules, or even different regions on the same type of macromolecules are likely to mediate adhesion of *Navicula* sp. I to mica and to Intersleek. Any of the above-mentioned mechanisms can be responsible for the observed variations in the value of unbinding forces and polymer extensions between the two surfaces, recorded with the same diatom classified as adhesive bioprobe (Figs. 5 and 7, *a* and *c*). It is apparent that the type of biopolymer-surface interactions contributing to the attachment of very adhesive diatoms (Figs. 7, *b* and *d*, and 9, *d–f*) to mica and to Intersleek differs from those seen for adhesive diatoms (Figs. 5, 7, *a* and *c*, and 9, *a–c*). This is also reflected in dissimilar values between the works of detachment calculated for these three bioprobes (Table 2).

In addition to raphe EPS, diatoms produce capsular exopolymer that comprises relatively thick polysaccharide-rich layers on the outer surface of the cell. Although the site of the origin and replenishment of capsule EPS is still undetermined, AFM measurements based on AFM tip-diatom cell surface interactions have shown that this soft, compressible material varies in its adhesiveness, with force values ranging from nonadhesive (0 pN), to moderately and very adhesive (~100 pN to 13–14 nN). Capsular polymer extensions range from ~200 nm to 2.5 μm, depending on diatom species (Higgins et al., 2003). The type of curves represented in Fig. 3 *f* could indicate the presence of capsular EPS on the cell surface. Whether motility, capsular, or both types of EPS contribute to the adhesion of *Navicula* to Intersleek and mica surfaces still remains to be determined.

CONCLUSIONS

The use of AFM with living marine diatoms of *Navicula* sp. I as bioprobes helped to evaluate the adhesive properties of EPS associated with individual cells on two materials dissimilar in physicochemical characteristics, such as mica and the silicone elastomer, Intersleek. The work of detachment of a single diatom from these surfaces, determined from force versus distance curves, using either the same or different diatoms in different growth phases, strongly depended on the individual *Navicula* cell and not on their growth stage. Despite these individual variations, diatoms could still be classified as nonadhesive, adhesive, and very adhesive, irrespective of the culture and the type of tested surface. Generally, comparable adhesion forces were measured on surfaces of hydrophobic Intersleek and hydrophilic mica, although subtle differences were noted in force versus extension distributions. The values and shapes of force versus distance curves supported the argument that the adhesion of *Navicula* sp. I to surfaces with different physicochemical properties is governed by macromolecular specificity of diatom EPS.

Whether the motility, capsular, or both types of EPS regulate *Navicula* adhesion to mica and Intersleek is still, however, a matter of speculation. The type of EPS macromolecules mediating cell adhesion also requires further elucidation.

Our study demonstrated that biological AFM with a live bioprobe can be successfully applied to carry out in situ characterization of cell adhesion to different surfaces. This is a promising method for the rapid assessment of diatom attachment to antifouling materials.

We gratefully acknowledge E. Holm and C. Belch (Naval Surface Warfare Center, Carderock Division) for preparation of the Intersleek coatings. We thank Nancy Equall, Angie Cheff, and James Monds for their contributions in SEM/EDX analysis and sample preparation.

This study was funded by the Office of Naval Research under grant No. N00014-02-1-063.

REFERENCES

Abu-Lail, N. I., and T. A. Camesano. 2002. Elasticity of *Pseudomonas putida* KT2442 surface polymers probed with single molecule force microscopy. *Langmuir*. 18:4071–4081.

Anonymous.1999. Intersleek 700: a new fouling control innovation from International. *Naval Architect*. June 1999:42.

Arce, F. T., R. Avci, I. B. Beech, K. E. Cooksey, and B. Wigglesworth-Cooksey. 2003. Microelastic properties of minimally adhesive surfaces: a comparative study of RTV11 and Intersleek elastomers. *J. Chem. Phys.* 119:1671–1682.

Bakker, D. P., F. P. Huijs, J. de Vries, J. W. Klijnstra, H. J. Busscher, and H. C. Van der Mei. 2003. Bacterial deposition to fluorinated and non-fluorinated polyurethane coatings with different elastic modulus and surface tension in a parallel plate and a stangnation point flow chamber. *Colloids Surf. B Biointerfaces*. 32:179–190.

Becker, K. 1996. Exopolysaccharide production and attachment strength of bacteria and diatoms on substrates with different surface tensions. *Microb. Ecol.* 32:23–33.

Beech, I. B., L. Hanjanksit, M. Kalaji, A. Neal, and V. Zinkevich. 1999. Exopolymer production by planktonic and biofilm *Pseudomonas* sp. NCIMB 2021 cells in continuous culture. *Microbiol.* 145:1491–1497.

Beech I. B., R. Gubner, V. Zinkevich, L. Hanjangsit, and R. Avci. 2000. Characterisation of conditioning layers formed by exopolymeric substances produced by Pseudomonas NCIMB 2021 on surfaces of AISI 304 and 316 stainless steel. *Biofouling*. 16:93–104.

Bowen, W. R., R. W. Lovitt, and C. J. Wright. 2001. Atomic force microscopy study of the adhesion of *Saccharomyces cervisiae*. *J. Colloid Interface Sci.* 237:54–61.

Callow, J. A., S. A. Crawford, M. J. Higgins, P. Mulvaney, and R. Wetherbee. 2000. The application of atomic force microscopy to topographical studies and force measurements on the secreted adhesive of the green algae *Enteromorpha*. *Planta*. 211:641–647.

Chamberlain, A. H. L. 1992. The role of adsorbed layers in bacterial adhesion. *In* Biofilms Science and Technology. L. F. Melo, T. R. Bott, M. Fletcher, and B. Capdeville, editors. Kluwer Academic, Dordrecht, The Netherlands. 59–67.

Characklis, W. G., and K. E. Cooksey. 1983. Biofilms and microbial fouling. Advances in applied microbiology. *Adv. Appl. Microbiol.* 29: 93–139.

Chiovitti, A., M. J. Higgins, R. E. Harper, and R. Wetherbee. 2003. The complex polysaccharides of the raphid diatom *Pinnularia viridis* (Bacillariophyceae). *J. Phycol.* 39:543–554.

Compere, C., M. N. Bellon-Fontaine, P. Bertrand, D. Costa, P. Marcus, C. Poleunis, C. M. Pradier, B. Rondot, and M. G. Walls. 2001. Kinetics of conditioning layer formation on stainless steel immersed in natural seawater. *Biofouling*. 17:129–145.

Cooksey, K. E. 1981. Requirement for calcium in the adhesion of a fouling diatom to glass. *Appl. Environ. Microbiol.* 41:1378–1382.

Cooksey, K. E., and H. Chansang. 1976. Isolation and physiological studies on 3 isolates of amphora (bacillariophyceae). *J. Phycol.* 12:455–460.

Cooksey, K. E., and B. Wigglesworth-Cooksey. 1995. Adhesion of bacteria and diatoms to surfaces in the sea: a review. *Aquat. Microb. Ecol.* 9: 87–96.

Crawford, S. A., M. J. Higgins, P. Mulvaney, and R. Wetherbee. 2001. Nanostructure of the diatom frustule as revealed by atomic force and scanning electron microscopy. *J. Phycol.* 37:543–554.

Dufrene, Y. F. 2000. Direct characterization of the physicochemical properties of fungal spores using functionalized AFM probes. *Biophys. J.* 78:3286–3291.

Dufrene, Y. F. 2001. Application of atomic force microscopy to microbial surfaces: from reconstituted cell surface layers to living cells. *Micron.* 32:153–165.

Finlay, J. A., M. E. Callow, L. K. Ista, G. P. Lopez, and J. A. Callow. 2002. The influence of surface wettability on the adhesion strength of settled spores of the green alga *Enteromorpha* and the diatom *Amphora*. *Integr. Comp. Biol.* 42:1116–1122.

Geesey, G. G. 1982. Microbial exopolymers: ecological and economic considerations. *ASM News*. 48:9–14.

Higgins, M. J., S. A. Crawford, P. Mulvaney, and R. Wetherbee. 2002. Characterization of the adhesive mucilages secreted by live diatom cells using atomic force microscopy. *Protist*. 153:25–28.

Higgins, M. J., J. E. Sader, P. Mulvaney, and R. Wetherbee. 2003. Probing the surface of living diatoms with atomic force microscopy: the nanostructure and nanomechanical properties of the mucilage layer. *J. Phycol.* 39:722–734.

Hinterdorfer, P., W. Baumgartner, H. J. Gruber, K. Schilcher, and H. Schindler. 1996. Detection and localization of individual antibody-antigen recognition events by atomic force microscopy. *Proc. Natl. Acad. Sci. USA*. 93:3477–3481.

Hoagland, K. D., J. R. Rowoski, M. R. Gretz, and S. C. Roener. 1993. Diatom extracellular polymeric substances:function, fine structure, chemistry and physiology. *J. Phycol.* 29:537–566.

Lind, J. L., K. Heimann, E. A. Miller, C. van Vliet, N. J. Hoogenraad, and R. Wetherbee. 1997. Substratum adhesion and gliding in a diatom are mediated by extracellular proteoglycans. *Planta*. 203:213–221.

Lower, S., M. F. Hochella, and T. J. Beveridge. 2001. Bacterial recognition of mineral surfaces: nanoscale interactions between *Schewanella* and α-FeOOH. *Science*. 292:1360–1363.

Marshall, K. C. 1992. Biofilms: an overwiew of bacterial adhesion, activity and control at surfaces. *ASM News*. 58:202–207.

Marszalek, P. E., H. B. Li, and J. M. Fernandez. 2001. Fingerprinting polysaccharides with single-molecule atomic force microscopy. *Nat. Biotechnol.* 19:258–262.

Neu, T. R., and K. C. Marschall. 1991. Microbial footprints, a new approach to adhesive polymers. *Biofouling*. 3:101–112.

Ong, Y.-L., A. Razatos, G. Georgiou, and M. M. Sharma. 1999. Adhesion forces between *E. coli* bacteria and biomaterial surfaces. *Langmuir*. 15:2719–2725.

Paul, J. H., and W. H. Jeffrey. 1985. Evidence for separate adhesion mechanisms for hydrophilic and hydrophobic surfaces in *Vibrio proteolytica*. *Appl. Environ. Microbiol.* 50:431–437.

Razatos, A., Y.-L. Ong, M. M. Sharma, and G. Georgiou. 1998. Molecular determinants of bacterial adhesion monitored by atomic force microscopy. *Proc. Natl. Acad. Sci. USA*. 95:11059–11064.

Schneider, P. R. 1997. Bacterial adhesion to solid substrata coated with conditioning films derived from chemical fractions of natural water. *J. Adhes. Sci. Technol.* 11:979–994.

Staats, N., B. de Winder, L. J. Stal, and L. R. Mur. 1999. Isolation and characterisation of extracellular polysaccharides from the epipelic diatoms *Cylindrotheca closterium* and *Navicula salinarum*. *Eur. J. Phycol.* 34:161–169.

Vadilli-Rodriguez, V., H. J. Busscher, W. Norde, J. De Vries, and H. C. Van der Mei. 2003. On relationship between microscopic and macroscopic physicochemical properties of bacterial cell surfaces: an AFM study on *Streptococcus mitis* strains. *Langmuir*. 19:2372–2377.

Van der Aa, B. C., and Y. Dufrene. 2002. In situ characterisation of bacterial extracellular polymeric substances by AFM. *Colloids Surf. B Biointerfaces*. 23:173–182.

van der Aa, B. C., M. M. Romain, M. Asther, M. T. Zamora, P. G. Rouxhet, and Y. F. Dufrene. 2001. Stretching cell surface macromolecules by atomic force microscopy. *Langmuir*. 17:3116–3119.

Van der Mei, H., H. J. Busscher, R. Bos, J. de Vries, C. J. P. Boonaert, and Y. Dufrene. 2000. Direct probing by atomic force microscopy of the cell surface softness of a fibrillated and nonfibrillated oral streptococcal strain. *Biophys. J.* 78:2668–2674.

Wetherbee, R., J. L. Lind, and J. Burke. 1998. The first kiss: establishment and control of initial adhesion by raphid diatoms. mini review. *J. Phycol.* 34:9–15.

Wigglesworth-Cooksey, B., D. Berglund, and K. E. Cooksey. 2001. Cell-cell and cell-surface interactions in an illuminated biofilm: Implications

for sediment stabilization. E-journal: *Geochem Trans*. 75–83 (article 10): http//www.rsc.org/is/journals/current/geochem/contents/lists/2001/gt001001.htm.

Wigglesworth-Cooksey, B., and K. E. Cooksey. 1992. Can diatom sense surfaces? State of our knowledge. *Biofouling*. 5:227–238.

Wigglesworth-Cooksey, B., and K. E. Cooksey. 2004. Involvement of calcium- based signal transduction and fluxes in biofilm formation and cellular dispersal by benthic marine diatoms. Proc. Annual Amer. Soc. Microbiol. (ASM) Meeting, Abstract Q210.

Wigglesworth-Cooksey, B., and K. E. Cooksey. 2005. Use of florescently conjugated lectins to study cell-cell interactions in model marine biofilms. *Appl. Environ. Microbiol.* In Press.

Wingender, J., T. R. Neu, and H.-C. Flemming. 1999. Microbial Extracellular Polymeric Substances: Characterization, Structure and Function: Springer-Verlag, Berlin.

Wustman, B. A., M. R. Gretz, and K. D. Hoagland. 1997. Extracellular matrix assembly in diatoms (*Bacillariophyceae*).1. A model of adhesives based on chemical characterization and localization of polysaccharides from the marine diatom Achnanthes longipes and other diatoms. *Plant Physiol*. 113:1059–1069.

Zinkevich, V., I. Bogdarina, H. Kang, M. A. W. Hill, R. Tapper, and I. B. Beech. 1996. Characterisation of exopolymers produced by different isolates of marine sulphate-reducing bacteria. *Int. Biodeterior. Biodegradation*. 37:163–172.